Apoptosis (2012) 17:25–36
DOI 10.1007/s10495-011-0653-6

ORIGINAL PAPER

Pterostilbene protects vascular endothelial cells against oxidized low-density lipoprotein-induced apoptosis in vitro and in vivo

Lu Zhang · GuangZhou Zhou · Wei Song · XiaoRong Tan · YuQi Guo · Bo Zhou · Hongjuan Jing · SuJuan Zhao · LiangKe Chen

Published online: 18 September 2011

Abstract Vascular endothelial cell (VEC) apoptosis is the main event occurring during the development of atherosclerosis. Pterostilbene (PT), a natural dimethylated analog of resveratrol, has been the subject of intense research in cancer and inflammation. However, the protective effects of PT against oxidized low-density lipoprotein (oxLDL)-induced apoptosis in VECs have not been clarified. We investigated the anti-apoptotic effects of PT in vitro and in vivo in mice. PT at 0.1–5 μM possessed antioxidant properties comparable to that of trolox in a cell-free system. Exposure of human umbilical vein VECs (HUVECs) to oxLDL (200 μg/ml) induced cell shrinkage, chromatin condensation, nuclear fragmentation, and cell apoptosis, but PT protected against such injuries. In addition, PT injection strongly decreased the number of TUNEL-positive cells in the endothelium of atherosclerotic plaque from apoE$^{-/-}$ mice. OxLDL increased reactive oxygen species (ROS) levels, NF-κB activation, p53 accumulation, apoptotic protein levels and caspases-9 and -3 activities and decreased mitochondrial membrane potential (MMP) and cytochrome c release in HUVECs. These alterations were attenuated by pretreatment with PT. PT inhibited the expression of lectin-like oxLDL receptor-1 (LOX-1) expression in vitro and in vivo. Cotreatment with PT and siRNA of LOX-1 synergistically reduced oxLDL-induced apoptosis in HUVECs. Overexpression of LOX-1 attenuated the protection by PT and suppressed the effects of PT on oxLDL-induced oxidative stress. PT may protect HUVECs against oxLDL-induced apoptosis by downregulating LOX-1-mediated activation through a pathway involving oxidative stress, p53, mitochondria, cytochrome c and caspase protease. PT might be a potential natural anti-apoptotic agent for the treatment of atherosclerosis.

Keywords Apoptosis · Atherosclerosis · Lectin-like oxLDL receptor-1 · Oxidized low density lipoprotein · Pterostilbene · Vascular endothelial cell

L. Zhang (✉) · G. Zhou · W. Song · X. Tan · H. Jing · S. Zhao · L. Chen
College of Bioengineering, Henan University of Technology, Lianhua Street, Zhengzhou 450001, China
e-mail: chaperones@163.com

YuQ. Guo
Department of Obstetrics and Gynecology, The Third Affiliated Hospital of Zhengzhou University, Zhengzhou 450052, China

B. Zhou
State Key Laboratory of Applied Organic Chemistry, Lanzhou University, 222 Tianshui Street S., Lanzhou 730000, China

Introduction

Endothelial dysfunction is a driving force in the initiation and development of atherosclerosis [1]. Apoptosis is one of the central mechanisms leading to endothelial dysfunction and results in elimination of cells, enhanced vessel wall permeability, and increased coagulatory activity of vascular endothelial cells (VECs). These alterations induce atherosclerotic lesion rupture and later clinical complications [2, 3]. Therefore, inhibiting VEC apoptosis is a therapeutic strategy against atherosclerosis.

Although the development of atherosclerosis appears to be the result of multiple maladaptive pathways, a particularly important risk factor in the pathogenesis of atherosclerosis is oxidized low-density lipoprotein (oxLDL), which contributes to endothelial dysfunction [4]. Early studies revealed that the morphological changes of cultured VECs associated with oxLDL toxicity are similar to

those observed in the endothelium covering atherosclerotic lesions [5]. VECs internalize and degrade oxLDL through a unique receptor-mediated pathway, which mainly involves the lectin-like oxLDL receptor-1 (LOX-1), both in vitro and in vivo [6, 7]. OxLDL binding to LOX-1 induced apoptosis in VECs, which was associated with several critical steps, including generation of intracellular oxidative stress, NF-κB activation, decreased anti-apoptotic protein levels and reduced mitochondrial membrane potential (MMP) with concomitant release of cytochrome c and subsequent activation of caspase-9 and -3 [8, 9].

Pterostilbene (PT) is a naturally occurring analogue of resveratrol found in blueberries and several varieties of grapes [10, 11]. It possesses various pharmacologic activities, including anti-cancer, anti-inflammation, anti-oxidant, and anti-diabetes activities [12–14]. PT inhibited platelet-derived growth factor (PDGF)-BB-induced proliferation of vascular smooth muscle cells (VSMCs) and DNA synthesis [15], so PT might be a potential anti-proliferative agent for treating of atherosclerosis. Furthermore, PT may have anti-oxidant and anti-neoplastic activities as effective as those of resveratrol because of the structural similarity of the two agents [16].

Accumulating evidence suggests that resveratrol can inhibit oxLDL-induced apoptosis in VECs [17, 18]. Unfortunately, resveratrol has a low bioavailability to cells [19]. By contrast, PT has better oral adsorption and metabolic stability because it has only one hydroxyl group. The dimethylether structure of PT enhances its lipophilicity and thus increases its membrane permeability, which leads to improved pharmacokinetic profiles over resveratrol [20]. However, whether PT can inhibit oxLDL-induced VEC apoptosis remains unknown. We aimed to evaluate the effects of PT on oxLDL-induced apoptosis in VECs and its possible molecular mechanism(s) in the present study.

Materials and methods

Cell culture

Human umbilical vein vascular endothelial cells (HUVECs) were obtained in our laboratory as described [21]. Cells were cultured on gelatin-coated plastic dishes in M199 medium (Gibco, USA) supplemented with 20% fetal bovine serum (FBS; Hyclone Lab Inc USA) and 70 ng/ml fibroblast growth factor 2 (FGF-2) in a humidified incubator at 37°C with 5% CO_2 and used for experiments at not greater than passage 8. The identity of HUVECs was confirmed by their cobblestone morphology and strong positive immunoreactivity to von Willebrand factor.

LDL isolation and oxidation

Native LDL and oxLDL were prepared as described [22]. Briefly, human native LDL was isolated from human plasma by sequential ultracentrifugation. LDL (2 mg protein/ml) was oxidized by exposure to 10 μM $CuSO_4$ for 24 h at 37°C. The extent of oxidation was determined by measuring the amount of thiobarbituric acid-reactive substances.

Cell viability assay

HUVECs were plated in 96-well cell culture plates. PT (Sigma-Aldrich, USA) was dissolved in dimethyl sulfoxide (DMSO). When cells were grown to 80% confluency, they were washed once with basal M199 medium, incubated with concentrations of PT for 2 h, then stimulated with oxLDL (200 μg/ml) for 24 or 48 h. Cell viability was determined by MTT assay as described [23]. The viability (%) was expressed as = (optical density [OD] of treated group/OD of control group) × 100%. The viability of the control group was set to 100%.

Analysis of apoptotic cells

The morphological changes in nuclei were detected by staining with acridine orange (AO, Sigma, USA). Cells were divided into four groups for treatment: control, incubation with DMSO < 0.1% (v/v); PT, incubation with 1 μM PT; oxLDL, incubation with 200 μg/ml oxLDL; PT + oxLDL, pretreatment with 1 μM PT for 2 h, then incubation with oxLDL. After treatment, cells in the four groups were stained with AO for 5 min and observed by confocal laser scanning microscopy (CLSM, Leica, Germany). Chromatin condensation was detected by nuclear staining with Hoechst 33258 (Sigma, USA). Briefly, cells were fixed with 2% formaldehyde for 10 min, stained with phosphate-buffered saline (PBS)/0.1% TritonX-100/10 μM Hoechst 33258 for 5 min, then were visualized by fluorescence microscopy (Nikon, Japan). Apoptotic cells are stained bright blue because of their chromatin condensation. In addition, apoptotic cells were assessed by terminal deoxynucleotidyl transferase-mediated dUTP nick endlabeling (TUNEL, Promega, USA) according to the manufacturer's protocol. Cells were evaluated by CLSM. The apoptosis rate was quantified by the TUNEL-positive rate.

Antioxidant activity assays

The antioxidant activity of PT at 0.1, 0.5, 1, 5 μM was measured in a cell-free system by OxiSelect™ oxygen radical antioxidant capacity (ORAC) and hydroxyl RAC (HORAC) assays (Cell Biolabs, Inc.). The values of ORAC

were expressed as relative trolox equivalent (TE) and HORAC as relative gallic acid equivalent (GAE). Results are expressed as means of triplicate results in three independent measurements.

Measurement of ROS levels

Intracellular ROS levels were determined by use of 2′,7′-dichlorofluorescin (DCHF) (Sigma, USA), which could be oxidized into DCF by intracellular ROS when entering into cells. ROS assay was performed as described [24]. ROS levels were quantified with the software for the CLSM. Results are shown as mean fluorescence intensity.

Measurement of antioxidant enzyme activities

To investigate the effect of PT on antioxidant enzyme activity after oxLDL stimulation, superoxide dismutase (SOD) and catalase activities in the homogenate were determined by an enzymatic assay method with commercial kits (Calbiochem) according to the manufacturer's instructions. Enzyme activity was converted to units/mg protein.

Immunofluorescence

After treatment, HUVECs were fixed in 4% paraformaldehyde (w/v) for 30 min at room temperature and blocked in 1 × PBS, 0.01% Triton X-100 (v/v) and 5% goat serum (v/v). Cells were subsequently incubated with anti-p65 or anti-LOX-1 antibodies (both Santa Cruz Biotechnology) overnight at 4°C, then rinsed in 1 × PBS three times and incubated with Alexa Fluor 488 goat anti-rabbit IgG (Zhongshan Biological Technology) for 1 h at room temperature. For negative controls, cells were incubated with normal IgG. CLSM involved a Leica TCS SP2 AOBS, with excitation at 488 nm, and the Leica Confocal Software (Leica Lasertechnik GmbH). Different fields of view (>3 regions) were analyzed for each labeling condition, and representative results are shown.

Western blot analysis

Cells with various treatments were lysed in protein lysis buffer (1% SDS in 25 mM Tris–HCl, pH 7.5, 4 mM EDTA, 100 mM NaCl, 1 mM PMSF, 10 μg/ml leupeptin and 10 μg/ml soybean trypsin inhibitor). Nuclear extracts of the endothelial protein were isolated by use of NE-PER nuclear and cytoplasmic extraction reagents (Thermo Fisher Scientific). The protein concentration was determined by Coomassie brilliant blue protein assay. Total or nuclear endothelial protein extracts (30 μg) were applied to 12% SDS–polyacrylamide gel and transferred to a nitrocellulose membrane (Millipore, USA). Blots were incubated with anti-p53, anti-Bax, anti-Bcl-2, anti-cytochrome c, anti-LOX-1, anti-p65, anti-β-actin or anti-lamin B1 antibodies (all Santa Cruz Biotechnology) and then with a horseradish peroxidase (HRP)-conjugated secondary antibody (Santa Cruz Biotechnology). Band intensity was quantified by use of Quantity one software. Total protein expression was normalized to β-actin levels, and nuclear protein expression was normalized to nuclear lamin B1 levels.

MMP measurement

MMP was estimated by fluorescence of JC-1 (Invitrogen) aggregates that are formed as a function of inner MMP. The formation of JC-1 aggregates and their fluorescence responds linearly to an increase in membrane potential. After treatment, HUVECs plated on 24-well plates were incubated with 4 μg/ml JC-1 for 15 min at 37°C in a humidified incubator, washed two times with PBS, and detected by fluorescence (for red fluorescence: excitation, 543 nm; emission, 600 nm; for green fluorescence: excitation, 488 nm; emission, 535 nm). We randomly selected the region of interest (ROI), and then zoomed in the same frames. Data are presented as ratio of red to green fluorescenc. Determination of MMP involved FACScan flow cytometry (BD FACSCalibur) [25].

Measurement of caspase-3 and caspase-9 activity

The activities of caspase-3 and -9 were measured according to the kit manufacturers' instructions. Briefly, after treatment, HUVECs were removed from culture dishes, washed twice with PBS, and pelleted by centrifugation. Cell pellets were then treated for 10 min with iced lysis buffer supplied with the caspase-3 and -9 assay kits (Calbiochem). Then the suspensions were centrifuged at 10000 g for 10 min, and the supernatants were transferred to a clear tube. The specific substrate conjugate [acetyl-Asp-Glu-Val-Asp-p-nitroaniline (Ac-DEVD-p-NA) for caspase-3 and acetyl-Leu-Glu-His-Asp-p-nitroaniline (Ac-LEHD-p-NA) for caspase-9] was added, and tubes were incubated at 37°C for 2 h. During incubation, the caspases cleaved the substrates to form p-NA. Caspase-3 and -9 activities were read in a microtiter plate reader at 405 nm.

RNA interference of LOX-1

LOX-1 was knocked down by an RNA interference (RNAi) following a small-interfering siRNA transfection protocol provided by Santa Cruz Biotechnology. HUVECs at 60% confluence were transfected with scramble RNA (negative

control) or siRNA against LOX-1 by the RNAiFect Transfection Reagent method (QIAGEN). After cells were transfected for 48 h, the medium was replaced with normal M199 medium, and cells were treated with PT, oxLDL, or their combination. The effect of gene silencing was monitored by western blot analysis.

Overexpression of LOX-1

pcDNA5 plasmids containing full-length human LOX-1 cDNAs (Origene Technologies, USA) or corresponding empty vectors were transfected into HUVECs by the Lipofectamine 2000 method (Invitrogen). We monitored the effect of overexpression 24 or 48 h after transfection by western blot analysis.

Animals and treatment

Male apoE$^{-/-}$ mice (B6.129P2-Apoetm1Unc/J, stock no. 002052) in a C57BL/6 background were obtained from the Department of Laboratory Animal Science, Peking University Health Science Center (PUHSC), China. All procedures were in accordance with the Guide for the Care and Use of Laboratory Animals published by the US National Institutes of Health (NIH Publication No. 85-23, revised 1996). Mice were given free access to an atherogenic diet (containing 21% fat and 0.15% cholesterol). To analyze the impact of PT on LOX-1 endothelial expression, mice at 32 weeks of age were divided into four groups ($n = 10$ per group): the first group was terminated to determine the extent of baseline established lesions; the second and third groups received intraperitoneal injections of PT (PT-HD, 20 mg/kg/day or PT-LD, 5 mg/kg/day); and the fourth control group was injected with the same volume (150 μl) of DMSO. Fresh PT was dissolved in DMSO and prepared daily. The treatment was provided for 8 weeks and was well tolerated. The study design is in Fig. 2a.

Tissue collection and double immunofluorescence

For mice at 32 and 40 weeks of age, food was removed for an 8-h fast. Following the fast, the animals were euthanized by exsanguination. The hearts and aortas were rapidly removed after perfusion with ice-cold PBS. The adventitia was thoroughly stripped, and the heart, including the aortic root, was snap-frozen in optimal cutting temperature (OCT) embedding medium (Tissue-Tek) for double immunofluorescence. Serial 7-μm-thick cryo-sections were collected from every three sections and mounted on poly-D-lysine-coated slides. In total, 20–40 sections were collected for each mouse. Sections were incubated with monoclonal anti-mouse endothelial cell antibody (CD31/PECAM-1, Santa Cruz Biotechnology), then monoclonal anti-mouse LOX-1 antibody (R&D Systems) for 1 h each. The negative control was the respective nonimmune IgGs (Santa Cruz Biotechnology). A mixture of goat anti-rat Alexa 488 and goat anti-rabbit Alexa 594 (Zhongshan Biological Technology) was applied for 30 min. Slides were observed by CLSM. To characterize endothelial cell apoptosis in the aortic roots of apoE$^{-/-}$ mice, sections were stained with CD31 antibodies and analyzed by use of the FragEL DNA Fragmentation Kit for TUNEL analysis. The sections were observed by CLSM, and TUNEL-positive cells colocalized with CD31-positive cells were counted in 100× fields of all sections from the aortic root of each animal.

Statistical Analyses

All experiments were performed in duplicate and repeated at least three times. Data are expressed as means ± SE. Treatment groups were compared by one-way variance (ANOVA) with SPSS 17.0 (SPSS Inc., Chicago) version. Differences were considered statistically significant at $P < 0.05$.

Results

PT inhibited oxLDL-induced cytotoxicity and apoptosis in VECs in vitro and in vivo

First, we evaluated the protective effects of PT (0.1–5 μM) by its antioxidant capacity in a cell-free system with ORAC and HORAC assays. As shown in Table 1, the antioxidant capacity of 5 μM PT was equal to 3.64 ± 1.59 μM TE and 12.86 ± 2.64 μM GAE. PT at 0.1, 0.5 and 1 μM had similar antioxidant activity as TE, but with HORAC, the antioxidant effect of PT was not detectable.

Phase-contrast microscopy was used to evaluate the effect of PT on morphological features of cultured HUVECs exposed to oxLDL. Incubating HUVECs with a cytotoxic concentration of oxLDL (200 μg/ml) for 24 or 48 h increased the number of shrinking cells and cells detached from the culture dish as compared with the control. Pretreatment with PT for 2 h then exposure to oxLDL

Table 1 The antioxidant activity of PT in a cell-free system

PT (μM)	ORAC (μM) TE	HORAC (μm)AE
5	3.64 ± 159	1256 ± 2.64
1	1.08 ± 042	ND
0.5	0.75 ± 0.27	ND
0.1	0.42 ± 030	ND

Results are means ± SE of three independent measurements. *ND* not detectable

for 24 or 48 h repaired the cell morphologic features (Fig. 1a). MTT assay revealed that oxLDL (200 μg/ml) significantly reduced the viability of HUVECs. PT prevented the reduced cell viability induced by oxLDL in a concentration-dependent manner, with a peak at 1 μM (Fig. 1b). Therefore, all subsequent experiments involved 1 μM of PT in vitro.

The induction of apoptosis in oxLDL-treated HUVECs was detected with AO and Hochest 33258 staining and TUNEL assays. Cells incubated with 200 μg/ml oxLDL for 24 h showed the typical features of apoptosis, including chromatin condensation and nuclear fragmentation, which were strongly inhibited in PT-pretreated cells (Fig. 1c). The proportion of apoptotic cells was quantified by TUNEL assay (Fig. 1d). After exposure to oxLDL for 24 h, the percentage of TUNEL-positive cells, representing DNA fragmentation, was increased by 7-fold. In PT-pretreated cells, the proportion of TUNEL-positive cells was decreased. Treatment with PT (0.1–5 μM) alone did not affect HUVEC viability (data not shown).

To assess the biological significance of our findings in vivo, we tested the effect of PT on endothelial cell apoptosis in advanced atherosclerotic lesions in the aortic roots of apoE$^{-/-}$ mice. CLSM of sections from aortic roots of the four groups of apoE$^{-/-}$ mice revealed that PT injection strongly downregulated the number of TUNEL-positive cells in the endothelium as compared with the control (Fig. 2b).

PT suppressed the oxLDL-induced oxidative stress and NF-κB activation in HUVECs

To investigate whether the anti-apoptotic effects of PT could be attributed to reduced oxidative stress, we detected intracellular ROS levels in HUVECs by using DCHF as a fluorescent probe. ROS levels were higher in oxLDL-treated than control cells at 3, 6 or 12 h ($P < 0.05$ or $P < 0.01$; Fig. 3a), and the oxLDL-induced high levels of ROS were decreased in PT-pretreated cells. In accordance with these findings, PT pretreatment inhibited the oxLDL-induced suppression of SOD and catalase activity (Fig. 3b, c). PT may inhibit HUVEC apoptosis by suppressing intracellular oxidative stress.

Numerous studies have provided strong support for VEC apoptosis being induced by oxidative stress through activation of NF-κB [26, 27]. Next, we performed experiments aimed at evaluating whether the protective effects of PT were associated with NF-κB signaling. Although PT did

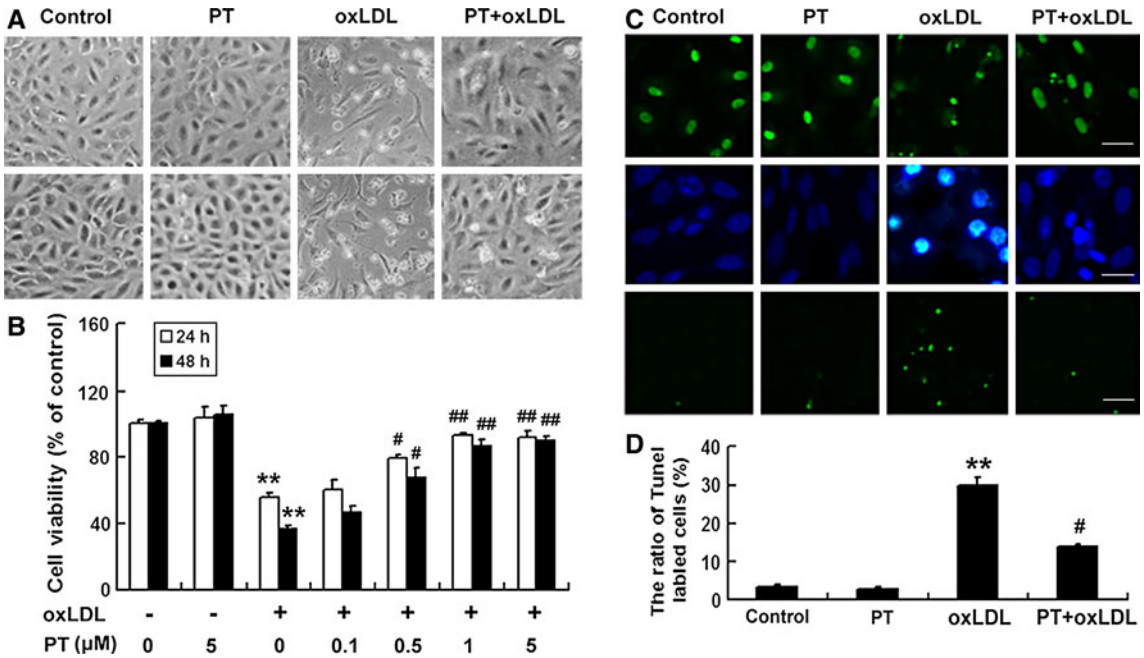

Fig. 1 Effect of pterostilbene on oxidized low-density lipoprotein (oxDL)-induced cytotoxicity and apoptosis in human umbilical vein endothelial cells (HUVECs). **a** Cells were incubated with oxLDL (200 μg/ml) with and without 1 μM PT for 24 or 48 h. Morphological micrographs obtained under a phase-contrast microscope (100×). Control, cells treated with 1 μM DMSO; PT, cells treated with 1 μM PT alone; oxLDL, cells treated with 200 μg/ml oxLDL; PT + oxLDL, after preincubation for 2 h with 1 μM PT, cells were treated with 200 μg/ml oxLDL. **b** Cell viability determined by MTT assay. $n = 3$, $^{**}P < 0.01$ versus Control, $^{\#}P < 0.05$ versus oxLDL, $^{\#\#}P < 0.01$ versus oxLDL. **c** Cell apoptosis was detected by acridine orange staining (*top*), Hochest 33258 staining (*middle*) and TUNEL assay (*bottom*) at 24 h. Fluorescence photographs were obtained under confocal laser scanning microscopy (CLSM) (AO staining and TUNEL assay) or fluorescence microscopy (Hochest 33258 staining). Bars = 40 μm. **d** Histogram shows the ratio of TUNEL-positive cells. $n = 3$, $^{**}P < 0.01$ versus control, $^{\#}P < 0.05$ versus oxLDL

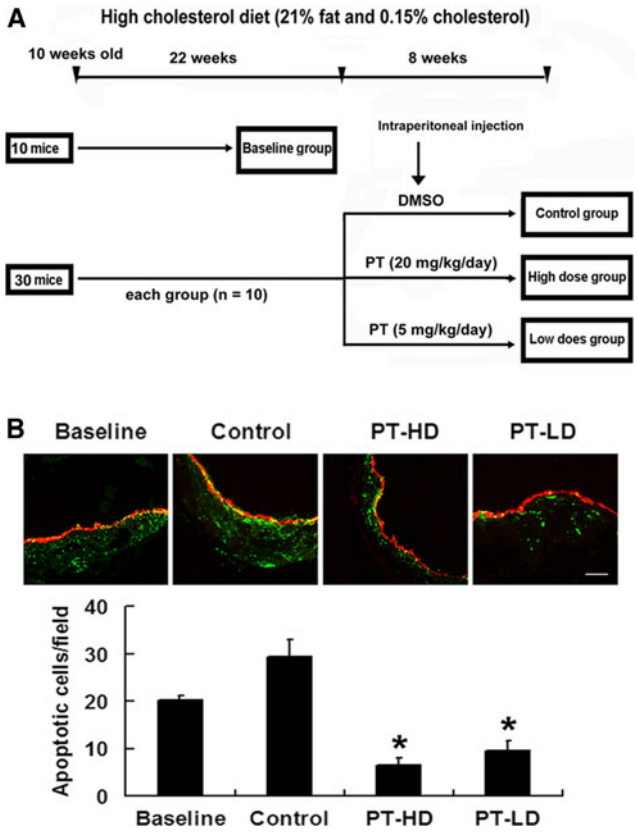

Fig. 2 Inhibitory effect of PT on VEC apoptosis in vivo in apoE$^{-/-}$ mice. **a** Experimental design of the four protocols for mice. **b** Double immunofluorescence photographs show apoptotic VECs (*green*) in the apoE$^{-/-}$ mouse aortic endothelium (CD31, *red*). Images are representative of a study conducted in a separate set of animals (each group, $n = 10$). Bar = 80 μm. ($n = 4$–5 sections for each sample). TUNEL-positive cells colocalized with CD31-positive cells were counted in low-power fields (100×) of all sections from the aortic root of each animal. Histogram shows the mean number of TUNEL-positive nuclei/field. *$P < 0.05$ versus control

not affect p65 distribution in control cells, it greatly prevented p65 nuclear translocation in oxLDL-treated HUVECs (Fig. 3d). Furthermore, pretreatment with PT significantly attenuated nuclear p65 level in oxLDL-treated cells as determined by western blot analysis (Fig. 3e). Pretreatment with the potent antioxidant *N*-acetylcystein (NAC) also blocked NF-κB activation.

PT inhibited the oxLDL-induced expression of apoptotic proteins and mitochondrial permeability transition in HUVECs

Several studies have demonstrated functional links between p53 expression and endothelial cell apoptosis through activation of NF-κB [27, 28]. Therefore, we examined the effects of PT on p53 levels in oxLDL-treated HUVECs. The level of p53 was upregulated in HUVECs incubated with oxLDL for 24 h as assessed by western blot analysis, whereas pretreatment with PT abolished the induction of p53 (Fig. 4a, b). Evidence indicated that p53 accumulation caused the activation of the pro-apoptotic protein Bax and reduced expression of the anti-apoptotic protein Bcl-2, thus leading to permeabilization of mitochondria and the release of cytochrome c and endothelial cell apoptosis [28]. Therefore, we investigated the effects of PT on p53-regulated intrinsic pro-apoptotic proteins and MMP. HUVECs incubated with oxLDL for 24 h showed increased Bax expression and decreased Bcl-2 levels (Fig. 4a, c). The MMP became depolarized in oxLDL-treated cells as indicated by the increase in green fluorescence and repression of red fluorescence. PT pretreatment contributed to the maintenance of MMP, as shown by repression of green fluorescence and restoration of red fluorescence (Fig. 4d). The results of flow cytometry supported these findings (Fig. 4e). Moreover, exposure of HUVECs to oxLDL induced the release of cytochrome c into the cytosolic fraction by 3.4 ± 0.47-fold higher than that of control cells; pretreatment with PT strongly blocked the oxLDL-p53-evoked pro-apoptotic protein expression and MMP level (Fig. 4).

PT sequentially suppressed the oxLDL-induced activation of caspase-9 and -3 in HUVECs

Bcl-2 can prevent the release of cytochrome c into cytosol, which is required to activate caspase-9 and -3 and subsequently induce cell apoptosis [29]. To confirm that pretreatment with PT actually inhibited oxLDL-induced apoptosis in HUVECs and whether PT performed its function by suppressing caspase-9 and -3 activation, we determined the activity of caspase-9 and -3 by colorimetric assay. OxLDL significantly upregulated the activity of caspase-9 and -3, and pretreatment with PT suppressed the activity of these apoptotic factors, which demonstrates that PT has an inhibitory effect on oxLDL-induced caspase activation and HUVEC apoptosis (Fig. 5).

PT's protection against oxLDL might be involved in LOX-1-mediated signaling in vitro and in vivo

LOX-1 is the major receptor for oxLDL and is mainly expressed by VECs. Therefore, we aimed to evaluate whether PT prevented the apoptotic signaling cascade by decreasing oxLDL-induced LOX-1 expression. Immunofluorescent staining (Fig. 6a) and western blot analysis (Fig. 6b) revealed that incubating HUVECs with oxLDL increased LOX-1 expression. Administration of PT significantly lowered such enhancement. Next, to study whether PT inhibits oxLDL-induced apoptosis by suppressing LOX-1-mediated signaling in HUVECs, we used knockdown of LOX-1 by siRNA and overexpressed LOX-1 by transfecting LOX-1 plasmids. Exposure of HUVECs to LOX-1

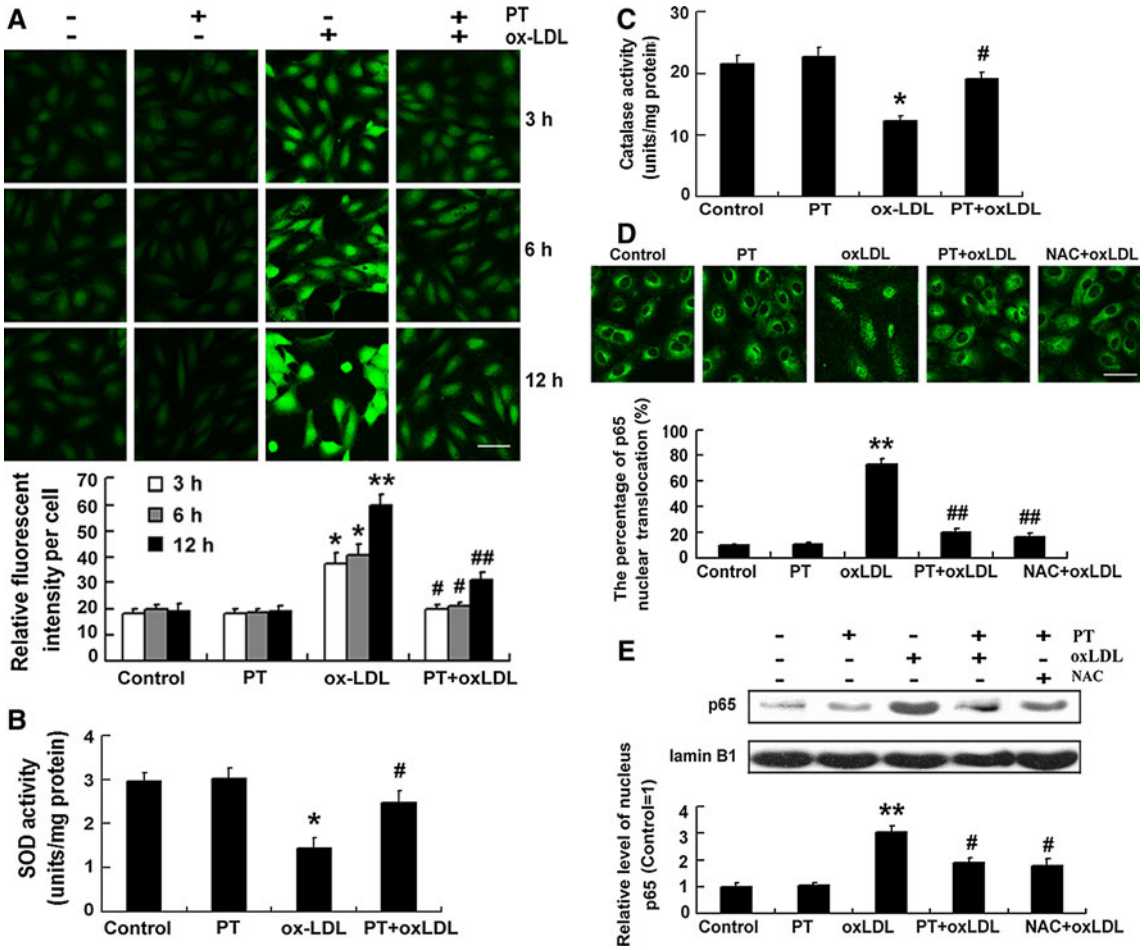

Fig. 3 Inhibitory effects of PT on oxLDL-induced oxidative stress and NF-κB activation in HUVECs. **a** Fluorescent images show intracellular levels of reactive oxygen species (ROS) in the four groups at 3, 6 or 12 h. Bar = 40 μm. Histogram shows the relative fluorescent intensity per cell determined by CLSM. Offset and gain values of the photomultiplier channel were regulated with respect to the set-up selected for control cells analysis to make fluorescence intensity comparable across experiments on different samples. $n = 3$, $^{*}P < 0.05$, $^{**}P < 0.01$ versus control, $^{\#}P < 0.05$, $^{\#\#}P < 0.01$ versus oxLDL. **b** The activity of SOD in HUVECs treated with oxLDL with or without 1 μM PT. $n = 3$, $^{*}P < 0.05$ versus control, $^{\#}P < 0.05$ versus oxLDL. **c** The activity of catalase in HUVECs treated with oxLDL with or without 1 μM PT. $n = 3$, $^{**}P < 0.05$ versus control, $^{\#\#}P < 0.05$ versus oxLDL. **d** PT or *N*-acetylcystein (NAC) pretreatment inhibited oxLDL-induced NF-κB (p65) nuclear localization in HUVECs. Bar = 40 μm. Histogram shows the proportion of p65 nuclear translocation. $n = 3$, $^{**}P < 0.01$ versus control, $^{\#\#}P < 0.01$ versus oxLDL. **e** Western blot analysis of the nuclear expression of p65 normalized to the levels of lamin B1. $n = 3$, $^{**}P < 0.01$ versus control, $^{\#}P < 0.05$ versus oxLDL

siRNA for 24 and 48 h decreased the levels of LOX-1 (Fig. 6c). Treatment with LOX-1 siRNA or PT alone did not induce cell apoptosis. Application of LOX-1 siRNA and PT, respectively, caused significant decreases, by 62% and 54%, in oxLDL-induced HUVEC apoptosis. Cotreatment with LOX-1 siRNA and PT reduced oxLDL-induced cell apoptosis by 83% (Fig. 6d, e). Furthermore, we confirmed the increased level of LOX-1 in pcDNA5-LOX-1 transfected HUVECs by western blot analysis; overexpression of LOX-1 attenuated PT-involved defense against oxLDL-induced apoptosis (Fig. 6d, f). In addition, we investigated whether PT inhibiting oxLDL-induced LOX-1 expression could lead to suppression of ROS levels in HUVECs. Overexpression of LOX-1 attenuated the effect of PT on high oxLDL-induced ROS levels (Fig. 6g). Thus, PT protected HUVECs against oxLDL-induced apoptosis, at least in part, by depressing LOX-1-mediated signaling.

To further elucidate whether PT treatment could attenuate LOX-1 expression in vivo, we injected DMSO, PT-HD (20 mg/kg/day) or PT-LD (5 mg/kg/day) into the peritoneal cavity of apoE$^{-/-}$ mice for 8 weeks. All mice appeared healthy and survived the treatment. Double-immunofluorescence staining revealed LOX-1 expression in the endothelial cell layer (CD31-positive cells) of advanced atherosclerotic lesions from the aortic roots of apoE$^{-/-}$ control mice, as we previously reported [30] (Fig. 7). The aortic roots of PT-treated groups revealed a reduced area of endothelium positively stained for LOX-1

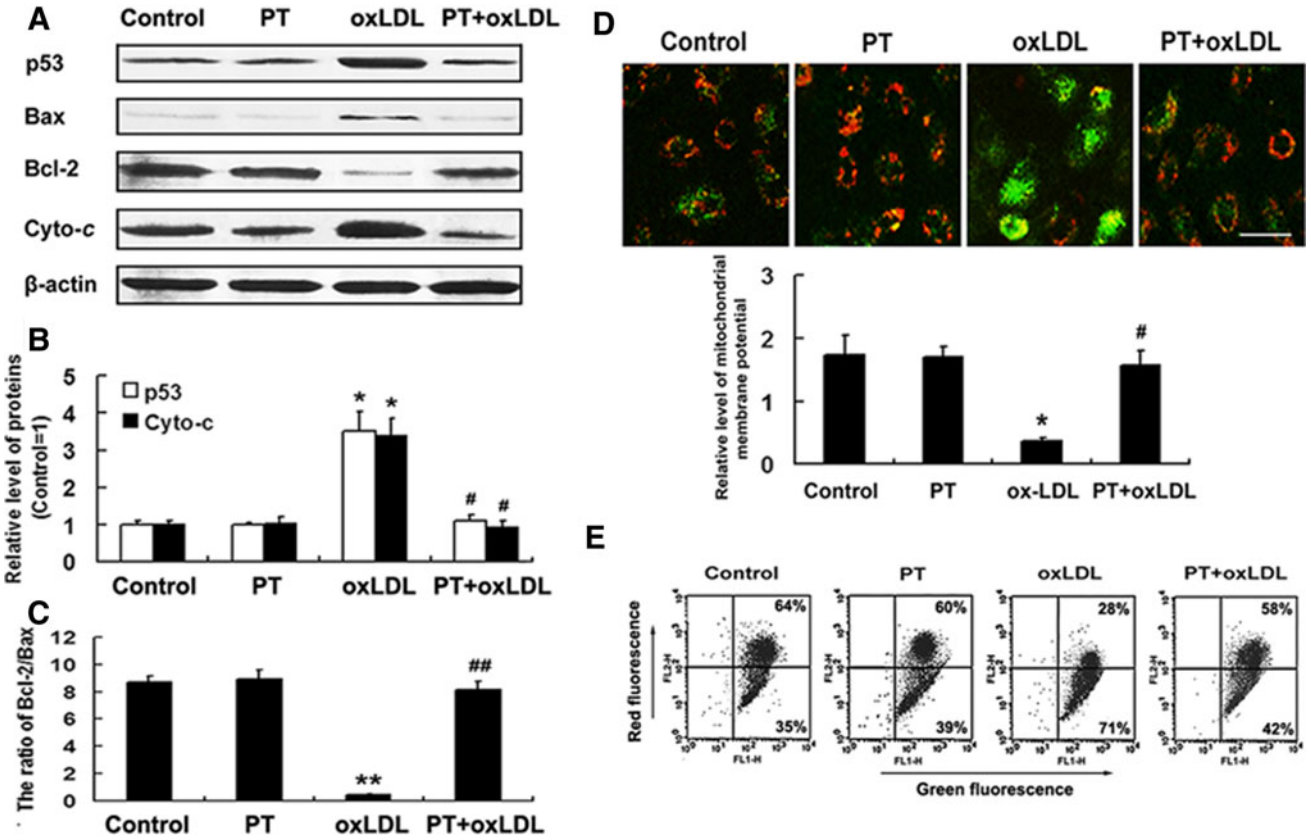

Fig. 4 Inhibitory effects of PT on oxLDL-induced apoptotic protein expression and mitochondrial permeability transition in HUVECs. **a** Western blot analysis of apoptosis-provoking proteins in response to oxLDL (200 μg/ml) and PT (1 μM) at 24 h. **b** Relative levels of p53 and cytochrome c (in the cytosolic fraction) normalized to levels of β-actin. $n = 3$, $^{*}P < 0.05$ versus control, $^{\#}P < 0.05$ versus oxLDL. **c** Ratio of Bcl-2 to Bax. $n = 3$, $^{**}P < 0.01$ versus control, $^{\#\#}P < 0.01$ versus oxLDL. **d** Matrix membrane potential (MMP) was tested with the fluorescent probe JC-1. Bar = 40 μm. Relative level of MMP was quantified by the relative ratio of red to green fluorescence intensity per cell. $n = 3$, $^{*}P < 0.05$ versus control, $^{\#}P < 0.05$ versus oxLDL. **e** JC-1 fluorescence for MMP was confirmed by flow cytometry. Green fluorescence intensity indicates cells with low MMP, red fluorescence intensity indicates cells with stable MMP. Data show a representative experiment from three independent experiments

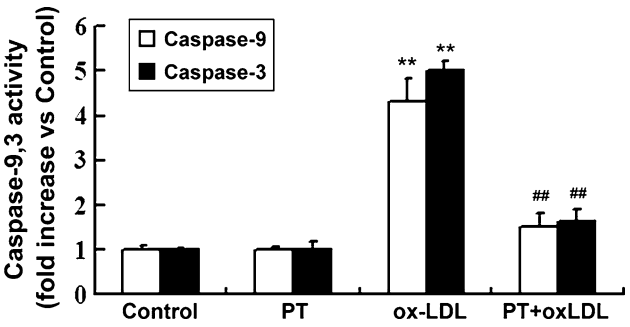

Fig. 5 Inhibitory effects of PT on oxLDL-induced caspase-9 and -3 activation. $n = 3$, $^{**}P < 0.01$ versus control, $^{\#\#}P < 0.01$ versus oxLDL

as compared with control aortic roots, which was consistent with the PT-induced downregulation of LOX-1 in oxLDL-treated HUVECs in vitro.

Discussion

Several observational epidemiologic studies have linked a diet rich in fruits and vegetables to low risk for cardiovascular disease [31, 32]. A hypothesized explanation for this finding is that these foods are rich in phytochemical, naturally occurring, non-nutritive substances that have disease preventive or protective properties. One such phytonutrient is resveratrol, a polyphenol synthesized by various plant species including grapes, which has demonstrated beneficial effects against cardiovascular diseases [33, 34]. VEC apoptosis, mainly induced by oxLDL, is commonly considered to have a pivotal role in atherosclerosis both in the early stages of lesion formation and later during disease development by inducing atherosclerotic plaque instability [35]. A therapeutically relevant mechanism by which resveratrol exerts its antiatherosclerotic tendency is protecting endothelial cells against oxLDL-induced apoptosis [36]. PT, a naturally

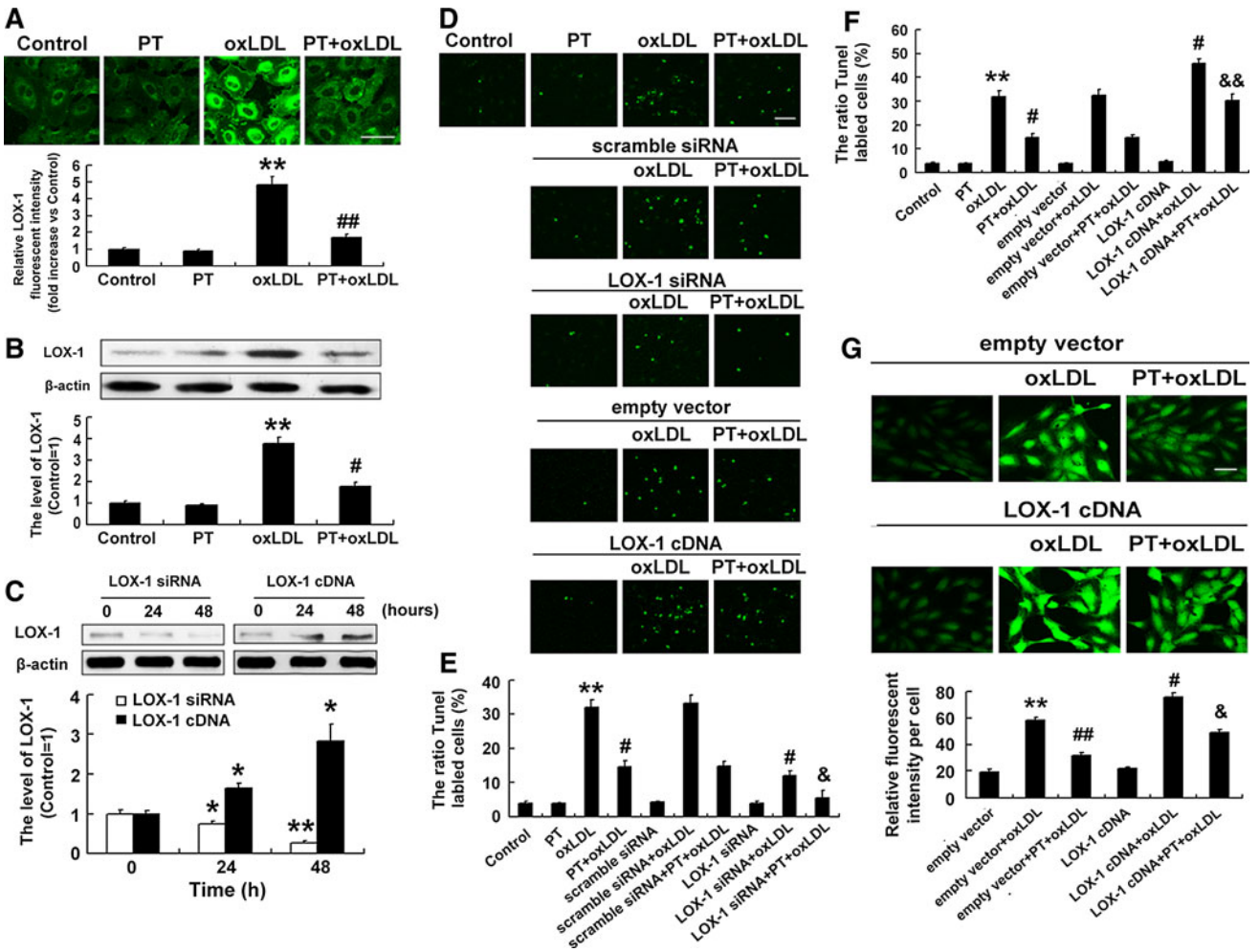

Fig. 6 Roles of LOX-1 in PT-involved cell protection. **a** Cells were incubated with oxLDL (200 μg/ml) with or without 1 μM PT for 24 h. Fluorescent images showed LOX-1 levels in the four groups. Bar = 40 μm. Histogram shows the relative fluorescent intensity per cell determined by CLSM. $n = 3$, $^{**}P < 0.01$ versus control, $^{\#\#}P < 0.01$ versus oxLDL. **c** Western blot analysis of LOX-1 levels normalized to the levels of β-actin. $n = 3$, $^{**}P < 0.01$ versus control, $^{\#}P < 0.05$ versus oxLDL. **c** HUVECs were treated with LOX-1 siRNA (*left*) or LOX-1 full-length cDNA (*right*), and the amount of cellular LOX-1 was detected by western blot. LOX-1 levels were normalized to levels of β-actin. $n = 3$, $^{*}P < 0.05$, $^{**}P < 0.01$ versus 0. **d** Effect of LOX-1 siRNA or LOX-1 full-length cDNA on PT protection by TUNEL assay. Fluorescence photographs were obtained by CLSM. Bar = 40 μm. **e** Cotreatment with PT and LOX-1 siRNA synergistically reduced oxLDL-induced apoptosis in HUVECs. $n = 3$, $^{**}P < 0.01$ versus control, $^{\#}P < 0.05$ versus oxLDL, $^{\&}P < 0.05$ versus PT + oxLDL. **f** Overexpression of LOX-1 by transfecting LOX-1 full-length cDNA significantly attenuated the PT protection against oxLDL-induced apoptosis in HUVECs. $n = 3$, $^{**}P < 0.01$ versus control, $^{\#}P < 0.05$ versus oxLDL, $^{\&\&}P < 0.01$ versus PT + oxLDL. **g** Overexpression of LOX-1 in HUVECs reversed the inhibitory effects of PT on oxLDL-induced ROS production. Bar = 40 μm. $n = 3$, $^{**}P < 0.01$ versus empty vector, $^{\#}P < 0.05$, $^{\#\#}P < 0.01$ versus empty vector + oxLDL, $^{\&}P < 0.05$ versus empty vector + PT + oxLDL

occurring analog of resveratrol, has been found more stable and potent than resveratrol [37]. However, whether PT could inhibit oxLDL-induced VEC apoptosis has not been studied. In this study, MTT assay showed that pretreatment with PT could effectively suppress the reduced cell viability induced by oxLDL. Furthermore, chromatin condensation and nuclear fragmentation were greatly inhibited in oxLDL-treated cells with PT pretreatment. Intraperitoneal injection of PT strongly downregulated the number of TUNEL-positive VECs covering atherosclerotic plaques from apoE$^{-/-}$ mice. These data suggest that PT could inhibit oxLDL-induced VEC apoptosis both in vitro and in vivo. Notably, the minimal effective concentration of PT was lower than that of resveratrol for inhibiting oxLDL-induced VEC apoptosis in other studies [18, 38], so PT may provide useful information about VEC apoptosis and perhaps open the door to an innovative therapeutic drug for atherosclerosis.

To understand why PT could inhibit VEC apoptosis so effectively, we next investigated the underlying mechanism(s). Previous studies have revealed apoptosis in VECs with elevated intracellular ROS levels [39, 40]. Intracellular ROS levels are regulated by the balance between ROS

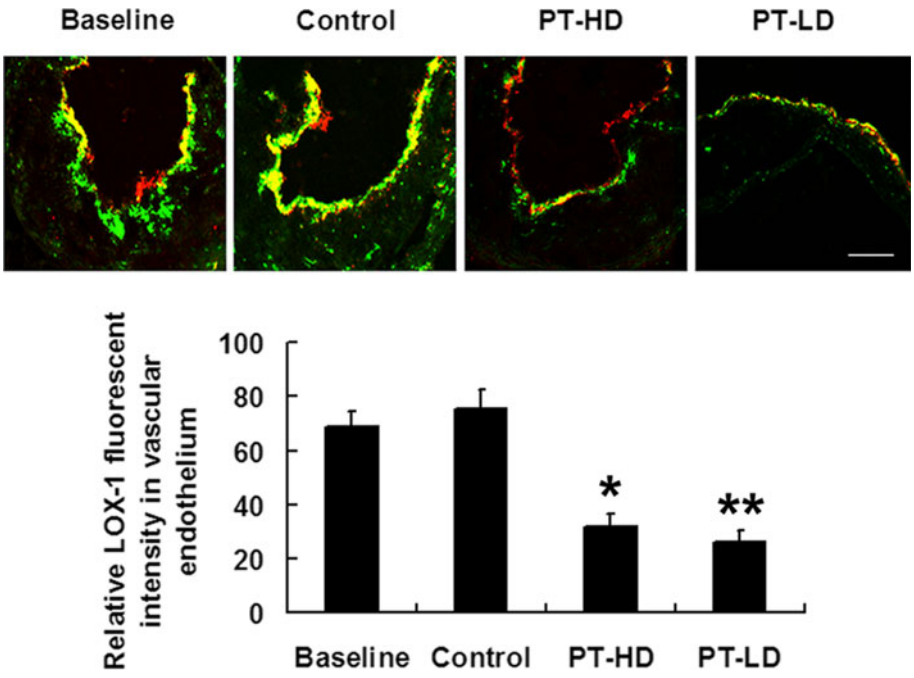

Fig. 7 Inhibitory effect of PT on endothelial LOX-1 expression in vivo. Double-stained images were merged to analyze colocalization (*yellow*) of LOX-1 (*green*) and CD31-positive VECs (*red*). Images are representative sections. ($n = 4$–5 sections per tissue, at least three sites of analysis per slide). Bar = 160 μm. Histogram shows the relative fluorescent intensity of LOX-1 in endothelium of apoE$^{-/-}$ mice (each group, $n = 10$). $^{*}P < 0.05$, $^{**}P < 0.01$ versus control

generation and antioxidant enzymes [41]. Our results showed that elevated ROS levels induced by oxLDL were decreased significantly with PT pretreatment. PT pretreatment reversed the oxLDL-induced reduction in SOD and catalase activities. In addition, PT (0.1–5 μM) possessed antioxidant properties comparable to trolox in a cell-free system. These data suggest that PT may protect against apoptosis by suppressing intracellular oxidative stress. OxLDL elicits vascular cell apoptosis by increasing ROS levels and the subsequent activation of NF-κB [42]. Once activated, NF-κB translocates from the cell cytosol to the nucleus and binds to specific DNA sequences and initiates transcription, thus resulting in changed gene expression, which is believed to be responsible for apoptosis [28]. We showed that PT decreased p65 nuclear translocation triggered by oxLDL. Pretreatment with NAC, a ROS scavenger, also blocked p65 nuclear translocation. Therefore, our results suggested that PT reduced the oxLDL-induced oxidative stress, which led to inhibited NF-κB activation. OxLDL-induced activation of NF-κB could increase the accumulation of p53 and expression of pro-apoptotic Bax and significantly decrease the expression of anti-apoptotic protein Bcl-2, thus leading to reduced MMP and the release of cytochrome c, which is critical for activation of the caspase cascade, the final common effector proteases mediating apoptosis signaling in VECs [27]. Our data showed that all these activities were alleviated by PT pretreatment. The mechanisms by which PT protects HUVECs against the apoptotic effects of oxLDL could be in part by upregulating the Bcl-2/Bax ratio and activating the mitochondrial signaling pathway.

OxLDL-induced apoptosis is mediated by the action of LOX-1 [9, 43]. We showed that oxLDL induced LOX-1 protein expression as was found previously [43, 44]; however, PT significantly inhibited such induction. Additionally, knocking down the translation of LOX-1 mRNA with siRNA promoted the PT-involved protection of VECs against oxLDL-induced apoptosis. In contrast, overexpression of LOX-1 in VECs attenuated the PT protection. Therefore, LOX-1 contributed to the PT protection against oxLDL-induced apoptotic insults to HUVECs. To further elucidate whether PT treatment could attenuate LOX-1 expression in vivo, we investigated the impact of PT in apoE$^{-/-}$ mice fed an atherogenic diet. Considering that the life span of mice is 2.5 years, 8 weeks of treatment represents approximately 6.6% of the life span of mice, so an 8-week course of treatment would be effective. LOX-1 levels were reduced in the atherosclerotic endothelium from the aortic roots of PT-treated mice, which was consistent with the PT-induced downregulation of LOX-1 in oxLDL-treated HUVECs in vitro. In parallel, overexpression of LOX-1 in VECs lessened the PT effect on high oxLDL-induced ROS levels. These findings indicate that PT inhibited oxLDL-induced apoptosis of HUVECs by inhibiting LOX-1 expression and receptor-mediated signal-transduction events. Previous studies have demonstrated that LOX-1 activation induces oxidative stress and in turn, stimulates LOX-1 expression [41, 45], which suggests a positive loop between oxidative stress and LOX-1 expression. Therefore, PT may inhibit LOX-1 expression by suppressing intracellular oxidative stress.

This is the first report to reveal the PT protection against atherogenic oxLDL-induced endothelial cell apoptosis. The

mechanisms are likely complex, and multiple signaling pathways may be involved in this process. One major mechanism underlying the anti-apoptotic effect of PT may be through inhibiting oxLDL-induced oxidative stress and subsequent NF-κB activation, which in turn activated the mitochondrion–cytochrome c–caspase protease pathway. The concentration of PT used in our study was similar to a previous report demonstrating that PT inhibited PDGF-BB–induced VSMC growth [15], but the minimal effective anti-apoptotic concentration of PT seemed to be relatively low as compared with resveratrol. Additionally, Ruiz et al. demonstrated that a high dose of PT (0–3000 mg/kg/day) in diet was not toxic in animals [46]. These data, coupled with the present findings, indicate that PT may have therapeutic effects for endothelial cell apoptosis-related and VSMC proliferation-related diseases such as atherosclerosis, restenosis after angioplasty and hypertension.

Acknowledgements This work was financially supported by the National Natural Science Foundation of China (no. 31101001), a doctoral scientific research start-up foundation from Henan University of Technology (nos. 2011BS013 and 2010BS016), and the Science and Technology Developmental Project of Zhengzhou (no. 20110942).

Conflict of interest The authors declare that they have no conflict of interest.

References

1. Libby P (2002) Inflammation in atherosclerosis. Nature 420: 868–874
2. Rajagopalan S, Somers EC, Brook RD, Kehrer C, Pfenninger D, Lewis E, Chakrabarti A, Richardson BC, Shelden E, McCune WJ, Kaplan MJ (2004) Endothelial cell apoptosis in systemic lupus erythematosus: a common pathway for abnormal vascular function and thrombosis propensity. Blood 103:3677–3683
3. Durand E, Scoazec A, Lafont A, Boddaert J, Al Hajzen A, Addad F, Mirshahi M, Desnos M, Tedgui A, Mallat Z (2004) In vivo induction of endothelial apoptosis leads to vessel thrombosis and endothelial denudation: a clue to the understanding of the mechanisms of thrombotic plaque erosion. Circulation 109:2503–2506
4. Liu S, Shen H, Xu M, Liu O, Zhao L, Liu S, Guo Z, Du J (2010) FRP inhibits ox-LDL-induced endothelial cell apoptosis through an Akt-NF-{kappa}B-Bcl-2 pathway and inhibits endothelial cell apoptosis in an apoE-knockout mouse model. Am J Physiol Endocrinol Metab 299:E351–E363
5. Ross R (1993) The pathogenesis of atherosclerosis: a perspective for the 1990 s. Nature 362:801–809
6. Chen J, Mehta JL, Haider N, Zhang X, Narula J, Li D (2004) Role of caspases in Ox-LDL-induced apoptotic cascade in human coronary artery endothelial cells. Circ Res 94:370–376
7. Kume N, Kita T (2001) Lectin-like oxidized low-density lipoprotein receptor-1 (LOX-1) in atherogenesis. Trends Cardiovasc Med 11:22–25
8. Chen XP, Xun KL, Wu Q, Zhang TT, Shi JS, Du GH (2007) Oxidized low density lipoprotein receptor-1 mediates oxidized low density lipoprotein-induced apoptosis in human umbilical vein endothelial cells: role of reactive oxygen species. Vascul Pharmacol 47:1–9
9. Li D, Mehta JL (2009) Intracellular signaling of LOX-1 in endothelial cell apoptosis. Circ Res 104:566–568
10. Mannal PW, Alosi JA, Schneider JG, McDonald DE, McFadden DW (2010) Pterostilbene inhibits pancreatic cancer in vitro. J Gastrointest Surg 14:873–879
11. Remsberg CM, Yáñez JA, Roupe KA, Davies NM (2007) High-performance liquid chromatographic analysis of pterostilbene in biological fluids using fluorescence detection. J Pharm Biomed Anal 43:250–254
12. Chen RJ, Ho CT, Wang YJ (2010) Pterostilbene induces autophagy and apoptosis in sensitive and chemoresistant human bladder cancer cells. Mol Nutr Food Res 54:1819–1832
13. Remsberg CM, Yáñez JA, Ohgami Y, Vega-Villa KR, Rimando AM, Davies NM (2008) Pharmacometrics of pterostilbene: preclinical pharmacokinetics and metabolism, anticancer, antiinflammatory, antioxidant and analgesic activity. Phytother Res 22:169–179
14. Pari L, Satheesh MA (2006) Effect of pterostilbene on hepatic key enzymes of glucose metabolism in streptozotocin- and nicotinamide-induced diabetic rats. Life Sci 79:641–645
15. Park ES, Lim Y, Hong JT, Yoo HS, Lee CK, Pyo MY, Yun YP (2010) Pterostilbene, a natural dimethylated analog of resveratrol, inhibits rat aortic vascular smooth muscle cell proliferation by blocking Akt-dependent pathway. Vascul Pharmacol 53(1–2):61–67
16. Cichocki M, Paluszczak J, Szaefer H, Piechowiak A, Rimando AM, Baer-Dubowska W (2008) Pterostilbene is equally potent as resveratrol in inhibiting 12-O-tetradecanoylphorbol-13-acetate activated NFkappaB, AP-1, COX-2, and iNOS in mouse epidermis. Mol Nutr Food Res 52(Suppl 1):S62–S70
17. Chang HC, Chen TG, Tai YT, Chen TL, Chiu WT, Chen RM (2011) Resveratrol attenuates oxidized LDL-evoked Lox-1 signaling and consequently protects against apoptotic insults to cerebrovascular endothelial cells. J Cereb Blood Flow Metab 31:842–854
18. Lin YL, Chang HC, Chen TL, Chang JH, Chiu WT, Lin JW, Chen RM (2010) Resveratrol protects against oxidized LDL-induced breakage of the blood-brain barrier by lessening disruption of tight junctions and apoptotic insults to mouse cerebrovascular endothelial cells. J Nutr 140:2187–2192
19. Asensi M, Medina I, Ortega A, Carretero J, Baño MC, Obrador E, Estrela JM (2002) Inhibition of cancer growth by resveratrol is related to its low bioavailability. Free Radic Biol Med 33: 387–398
20. Lin HS, Yue BD, Ho PC (2009) Determination of pterostilbene in rat plasma by a simple HPLC-UV method and its application in pre-clinical pharmacokinetic study. Biomed Chromatogr 23: 1308–1315
21. Jaffe EA, Nachman RL, Becker CG, Minick CR (1973) Culture of human endothelial cells derived from umbilical veins. Identification by morphologic and immunologic criteria. J Clin Invest 52:2745–2756
22. Hessler JR, Morel DW, Lewis LJ, Chisolm GM (1983) Lipoprotein oxidation and lipoprotein-induced cytotoxicity. Arteriosclerosis 3:215–222
23. Price P, McMillan TJ (1990) Use of the tetrazolium assay in measuring the response of human tumor cells to ionizing radiation. Cancer Res 50:1392–1396
24. Suematsu N, Tsutsui H, Wen J, Kang D, Ikeuchi M, Ide T, Hayashidani S, Shiomi T, Kubota T, Hamasaki N, Takeshita A (2003) Oxidative stress mediates tumor necrosis factor-alpha-induced mitochondrial DNA damage and dysfunction in cardiac myocytes. Circulation 107:1418–1423

25. Bedner E, Li X, Gorczyca W, Melamed MR, Darzynkiewicz Z (1999) Analysis of apoptosis by laser scanning cytometry. Cytometry 35:181–195
26. Liu X, Sun J (2010) Endothelial cells dysfunction induced by silica nanoparticles through oxidative stress via JNK/P53 and NF-kappaB pathways. Biomaterials 31:8198–8209
27. Aoki M, Nata T, Morishita R, Matsushita H, Nakagami H, Yamamoto K, Yamazaki K, Nakabayashi M, Ogihara T, Kaneda Y (2001) Endothelial apoptosis induced by oxidative stress through activation of NF-kappaB: antiapoptotic effect of antioxidant agents on endothelial cells. Hypertension 38:48–55
28. Ou HC, Lee WJ, Lee SD, Huang CY, Chiu TH, Tsai KL, Hsu WC, Sheu WH (2010) Ellagic acid protects endothelial cells from oxidized low-density lipoprotein-induced apoptosis by modulating the PI3 K/Akt/eNOS pathway. Toxicol Appl Pharmacol 248:134–143
29. Marsden VS, O'Connor L, O'Reilly LA, Silke J, Metcalf D, Ekert PG, Huang DC, Cecconi F, Kuida K, Tomaselli KJ, Roy S, Nicholson DW, Vaux DL, Bouillet P, Adams JM, Strasser A (2002) Apoptosis initiated by Bcl-2-regulated caspase activation independently of the cytochrome C/Apaf-1/caspase-9 apoptosome. Nature 419:634–637
30. Zhang L, Zhao J, Su L, Huang B, Wang L, Su H, Zhang Y, Zhang S, Miao J (2010) D609 inhibits progression of preexisting atheroma and promotes lesion stability in apolipoprotein e-/- mice: a role of phosphatidylcholine-specific phospholipase in atherosclerosis. Arterioscler Thromb Vasc Biol 30:411–418
31. Kushi LH, Meyer KA, Jacobs DR Jr (1999) Cereals, legumes, and chronic disease risk reduction: evidence from epidemiologic studies. Am J Clin Nutr 70:451S–458S
32. Dauchet L, Amouyel P, Dallongeville J, Medscape (2009) Fruits, vegetables and coronary heart disease. Nat Rev Cardiol 6: 599–608
33. Petrovski G, Gurusamy N, Das DK (2011) Resveratrol in cardiovascular health and disease. Ann N Y Acad Sci 1215:22–33
34. de la Lastra CA, Villegas I (2005) Resveratrol as an anti-inflammatory and anti-aging agent: mechanisms and clinical implications. Mol Nutr Food Res 49:405–430
35. Salvayre R, Auge N, Benoist H, Negre-Salvayre A (2002) Oxidized low-density lipoprotein-induced apoptosis. Biochim Biophys Acta 1585:213–221
36. Pendurthi UR, Williams JT, Rao LV (1999) Resveratrol, a polyphenolic compound found in wine, inhibits tissue factor expression in vascular cells: A possible mechanism for the cardiovascular benefits associated with moderate consumption of wine. Arterioscler Thromb Vasc Biol 19:419–426
37. Chiou YS, Tsai ML, Nagabhushanam K, Wang YJ, Wu CH, Ho CT, Pan MH (2011) Pterostilbene Is More Potent than Resveratrol in Preventing Azoxymethane (AOM)-Induced Colon Tumorigenesis via Activation of the NF-E2-Related Factor 2 (Nrf2)-Mediated Antioxidant Signaling Pathway. J Agric Food Chem 59:2725–2733
38. Ou HC, Chou FP, Sheen HM, Lin TM, Yang CH, Huey-Herng Sheu W (2006) Resveratrol, a polyphenolic compound in red wine, protects against oxidized LDL-induced cytotoxicity in endothelial cells. Clin Chim Acta 364:196–204
39. Yang Z, von Ballmoos MW, Faessler D, Voelzmann J, Ortmann J, Diehm N, Kalka-Moll W, Baumgartner I, Di Santo S, Kalka C (2010) Paracrine factors secreted by endothelial progenitor cells prevent oxidative stress-induced apoptosis of mature endothelial cells. Atherosclerosis 211:103–109
40. Irani K (2000) Oxidant signaling in vascular cell growth, death, and survival: a review of the roles of reactive oxygen species in smooth muscle and endothelial cell mitogenic and apoptotic signaling. Circ Res 87:179–183
41. Lee WJ, Ou HC, Hsu WC, Chou MM, Tseng JJ, Hsu SL, Tsai KL, Sheu WH (2010) Ellagic acid inhibits oxidized LDL-mediated LOX-1 expression, ROS generation, and inflammation in human endothelial cells. J Vasc Surg 52:1290–1300
42. Ou HC, Chou FP, Sheu WH, Hsu SL, Lee WJ (2007) Protective effects of magnolol against oxidized LDL-induced apoptosis in endothelial cells. Arch Toxicol 81:421–432
43. Lu J, Yang JH, Burns AR, Chen HH, Tang D, Walterscheid JP, Suzuki S, Yang CY, Sawamura T, Chen CH (2009) Mediation of electronegative low-density lipoprotein signaling by LOX-1: a possible mechanism of endothelial apoptosis. Circ Res 104: 619–627
44. Mattaliano MD, Huard C, Cao W, Hill AA, Zhong W, Martinez RV, Harnish DC, Paulsen JE, Shih HH (2009) LOX-1-dependent transcriptional regulation in response to oxidized LDL treatment of human aortic endothelial cells. Am J Physiol Cell Physiol 296:C1329–C1337
45. Cominacini L, Pasini AF, Garbin U, Davoli A, Tosetti ML, Campagnola M, Rigoni A, Pastorino AM, Lo Cascio V, Sawamura T (2000) Oxidized low density lipoprotein (ox-LDL) binding to ox-LDL receptor-1 in endothelial cells induces the activation of NF-kappaB through an increased production of intracellular reactive oxygen species. J Biol Chem 275:12633–12638
46. Ruiz MJ, Fernández M, Picó Y, Mañes J, Asensi M, Carda C, Asensio G, Estrela JM (2009) Dietary administration of high doses of pterostilbene and quercetin to mice is not toxic. J Agric Food Chem 57:3180–3186